ELSEVIER

Earth and Planetary Science Letters 200 (2002) 63–78

EPSL

www.elsevier.com/locate/epsl

Potassium in the Earth's core?

C.K. Gessmann *, B.J. Wood

Department of Earth Sciences, University of Bristol, Queens Road, Bristol BS8 1RJ, UK

Received 8 November 2001; received in revised form 5 March 2002; accepted 7 March 2002

Abstract

The partitioning of K and Na between liquid Fe–S–O alloys and silicate melt has been determined over the pressure and temperature range 2.5–24 GPa and 1500–1900°C. In experiments with S-free Fe alloys, the alkali elements show completely lithophile behaviour. When S is added, however, K and Na begin to enter the Fe-liquid phase and their distribution coefficients D_I ($=[I]_{metal}/[I]_{silicate}$) correlate strongly with O content (and FeO activity) of the Fe–S–O liquid and with the composition of the silicate melt. For potassium, D_K is $\sim$1.0 for Fe–sulphide liquid containing 30% S and 8% O. Increasing temperature leads to increasing O solubility in the Fe–sulphide liquid and correspondingly higher values of D_K. Increasing pressure on the other hand slightly reduces D_K values. Given a planetary core containing 10 wt% S and 4–8 wt% O, then several hundred ppm K would be present in the Fe–sulphide liquid if it segregated at low pressures, e.g. in a small planetary body such as Mars. If, as has recently been suggested, the Earth's core separated at the base of a deep magma ocean, then its highest possible K content is about 250 ppm. The latter would generate approximately 20% of the total heat production of the core. K can only be present in the core, however, if, at some time during its formation, a discrete O-rich FeS liquid separated from the silicate mantle. Finally, the sulphide compositions produced in our experiments imply that a combination of S and O could contribute significantly to the light element content of the Earth's core.

Keywords: potassium; density; dynamos; Earth; core; high pressure; iron sulfides

1. Introduction

One of the most important events in the history of the Earth was the separation of its iron-rich core from the silicate mantle. After core segregation the mantle was greatly depleted, relative to primitive planetary material, in siderophile elements and also in some elements which are not known to be siderophile. Among these, the alkali metals, in particular potassium, are of great importance. K and Na concentrations in the silicate earth are approximately 20% of those in primitive C1 chondrites and their depletion is generally ascribed to their volatility during the early phases of planetary accretion. On the other hand, it has also been suggested that at least part of the K deficit in the mantle may be due to extraction and segregation in S-rich liquid to the core (e.g. [1]). This hypothesis has profound implications for the history of the Earth. If correct it provides an addi-

* Corresponding author. Present address: Max-Planck Institut für Chemie, Hochdruck Mineralphysik, Postfach 3060, 55020 Mainz, Germany. Tel.: +49-6131-305-259; Fax: +49-6131-305-330.

E-mail address: gessmann@mpch-mainz.mpg.de (C.K. Gessmann).

0012-821X/02/$ – see front matter
PII: S0012-821X(02)00593-9

tional energy source (^{40}K) for the geodynamo. The hypothesis is supported by theoretical [2,3] and experimental evidence [4] indicating that K takes on a transition metal-like character at high pressures. The implication is that K could alloy with Fe and other transition metals under core conditions.

Assuming, for illustration, a C1 chondrite concentration of potassium in the bulk Earth ($\sim$550 ppm) and a primitive mantle concentration of 240 ppm K [5], then the content of K in the Earth's core would have to be $\sim$1200 ppm. This potassium would currently produce up to $\sim 8\times10^{12}$ W, which is about 20% of the total global heat loss [6] and possibly all the energy which is required to power the geodynamo. This quantity is not very well constrained, however, Gubbins et al. [7] give a maximum estimate of $\sim 10^{13}$ W (also [8]). Another important implication is that if K is indeed sufficiently chalcophile (or siderophile) to segregate into the core, then this may also have occurred on other planetary bodies, such as Mars or the Aubrite Parent Body.

Despite the important implications of K dissolution into the core, there are relatively few data on the partitioning of alkali elements between silicate and metallic phases under conditions relevant to core formation. 1 bar data and early low-pressure results (up to 1.5 GPa) indicate a range of $D_K^{\text{Fe–sulphide/silicate}}$ (= wt% K in Fe–sulphide alloy/wt% K in silicate melt) values from 1×10^{-4} to 0.03 which are summarised and presented in [9]. A recent systematic study by Chabot and Drake [10] yields almost the same range of D_K values (1.3×10^{4} to 0.037) at fixed pressure and temperature of 1.5 GPa and 1900°C. In the latter study the spread of the D_K values must be caused by one or more compositional variables, including the S and C contents of the Fe alloys and the degree of polymerisation of the silicate melt. At higher pressures available data are even more limited. Ohtani and co-workers [11,12] reported six metal–silicate distribution coefficients for K (0.08–0.36) and upper limits for D_{Na} in the pressure range 4–7 GPa. One experiment at 26 GPa [13] and another at 20 GPa [14] yielded D_K values of 0.015 and 0.24 respectively. All of the eight high-pressure experiments have, however, been criticised because of the small size of the Fe alloy phases, which may hamper accurate K analysis [10]. In summary, the available D_K data cover four orders of magnitude, providing almost no constraint on the K content of the core. The effects of bulk composition are, as illustrated by Chabot and Drake [10], large but have been neither properly quantified nor separated from the effects of pressure and temperature.

In this study we investigated the partitioning of the alkali metals K and Na between liquid Fe–S alloys and liquid silicate under conditions appropriate to core formation. The aim was to resolve the influences of compositional variables, pressure and temperature on alkali metal distribution behaviour. The results are interpreted with respect to K and Na partitioning in possible core formation scenarios and the potential heat production in the Earth's core due to the presence of K.

2. Experimental details

Liquid Fe alloys (S-bearing and S-free) were equilibrated with (K- and/or Na-bearing) silicate melt in a piston cylinder apparatus at 2.5 GPa. The mixed powders were contained in either MgO or quartz capsules, surrounded by crushable alumina and by a cylindrical graphite furnace. Pressed $BaCO_3$ was used as the pressure medium with a thin inner sleeve of silica glass to protect the charge from Ba contamination. All assembly components were fired at 1073 K, with the exception of the capsule, which was dried in a vacuum oven at 473 K overnight, and the graphite furnace, which was not heated. The temperature of the experiment was controlled by a $W_3Re/W_{25}Re$ thermocouple situated directly above the capsule. Pressure was applied gradually over a 10 min period together with a temperature ramp of 150–170 K/min to about 200 K below the target temperature. The final temperature was approached with a ramp rate of about 50 K/min and experimental duration, at temperature, was 30–80 min (Table 2). The experiments were quenched by turning off the power to the furnaces.

Experiments at higher pressures were performed in multianvil devices and involved equili-

brating Fe–sulphide alloys with silicate melt in MgO capsules. An 8 GPa experiment was performed in a 1000 tonne Walker-type multianvil press (e.g. [15]) with a pressure assembly consisting of a cast MgO octahedron (doped with 5 wt% Cr_2O_3) with integrated gasket fins and an edge length of 18 mm. A 24 GPa experiment was performed at the Bayerisches Geoinstitut, Bayreuth, Germany using an MgO (+5 wt% Cr_2O_3) octahedron with 10 mm edge length. Both multianvil pressure assemblies contained a cylindrical $LaCrO_3$ heater, surrounded by a zirconia sleeve. Temperature was monitored with a $W_3Re/W_{25}Re$ thermocouple located axially with respect to the heater and with the junction in direct contact with the MgO capsule. The *P–T* uncertainties are estimated to be ± 0.5 GPa and ± 40 K respectively. The octahedra were compressed using 25.4 and 32 mm tungsten carbide anvils (Toshiba grade F) with truncation edge lengths of 12 and 4 mm respectively. Pyrophyllite gaskets were used for the 24 GPa experiment. In each multianvil experiment, the sample was first compressed to the desired pressure; the temperature was then raised at ~ 100 K/min to the desired run temperature and then held there for 5–10 min (Table 2b). Gessmann and Rubie [16] show that runtimes exceeding 2–4 min are sufficient to reach equilibrium in similar experiments. The sample was quenched by switching off the power to the furnace and then slowly decompressed.

Starting materials were prepared from analytical grade metals, oxides, carbonates and chlorides. The metal composition was varied in the Fe–FeS–FeO–FeSi system (FeO mixed from appropriate amounts of Fe and Fe_2O_3). For the silicate starting materials (Table 1) K, Na and Ca were added as carbonates, the other major elements as oxides. A number of trace elements were added at 1000 ppm each by micropipetting of atomic absorption standard solutions (Table 1). The mixes were decarbonated by heating them in 100° steps between 500 and 1000°C. The synthetic silicate starting materials contain up to 10 wt% of K_2O and Na_2O. Although such alkali concentrations are much higher than their estimated bulk Earth contents, distribution coefficients of K are not correlated with the K concentration of the sample [10]. Therefore, present results can be extrapolated to Earth-like concentrations. Na-free silicate starting materials were used for most of the experiments because Na-bearing experiments strongly react with air therefore hampering accurate chemical analysis of the run products (for discussion see below). Some experiments were also performed with FeNi metal alloy (Fe:Ni 4:1 by weight) and addition of KCl and NaCl as sources for alkalis. Metal and silicate powders were usually mixed in a 1:1 weight ratio.

After the completion of each experiment, the entire sample assembly was mounted in epoxy, sectioned through the centre of the sample and then polished for electron microprobe analysis. The preparation of the sample was performed with oil-based lubricants for cutting, grinding and polishing, to avoid oxidation. The samples

Table 1
Composition of silicate and oxide starting materials

	Na-K-silicate (Sil)	K-silicate (K-Sil)	K-silicate+ (K-Sil+)	SiO_2+chloride
K_2O[a]	9.33	10.53	10.42	
Na_2O[a]	9.23			
MgO	17.58	22.38	22.14	
CaO[a]	12.82	14.09	13.94	
Fe_2O_3	2.81			
Al_2O_3	6.80	7.48	7.40	
SiO_2	41.43	45.53	45.05	75.0
HFSEs			1.10[b]	
KCl				12.5
NaCl				12.5

[a] Na, K and Ca were added as carbonates.
[b] 1000 ppm each of Li, Zn, Zr, Hf, Pb, Nd, Sm, Lu, Th, U, Nb were added.

Table 2a
Experimental conditions of piston cylinder experiments with S-free and S-poor starting materials

Run No.	T	P	Time	Starting materials		S content in metal liquid	K and Na content in quenched liquid Fe alloy
	(°C)	(GPa)	(min)	Fe alloy[a]	Silicate		
3	1600	2.5	65	$Fe_{75}FeO_{25}$	Sil	S-free	Below D.L.
11	1615	2.5	65	$FeNi_{50}FeS_{50}$	Sil[b]	S-free	Below D.L.
12	1700	2.5	60	FeNi	SiO_2+Chld.[b]	S-free[c]	Below D.L.
14	1700	2.5	50	$FeS_{50}FeNi_{50}$	SiO_2+Chld.[b]	8 wt%[c]	Below D.L.
18	1600	2.5	80	$FeS_{50}FeSi_{50}$	K-Sil	1 wt%	Below D.L./thin S-rich met. rim
19	1700	2.5	75	FeS_{50} $FeSi_{50}$	Sil	0.5 wt%	Below D.L.

Unless otherwise stated, metal and silicate powders were mixed in a 1:1 weight ratio. Unless stated otherwise, MgO capsules were used. Qtz = quartz; Below D.L. = below the detection limit. Sil = Na- and K-bearing starting material (Table 1); K-Sil = Na-free starting starting material (Table 1); SiO_2+Chld. = K- and Na-chloride-bearing starting material (Table 1).
[a] Subscripts give wt% of the respective component in the metal alloy.
[b] Metal–silicate ratio 4:1 (by weight).
[c] No Cl was detected in the quenched Fe alloy.

were analysed using a JEOL 8600 electron microprobe at the University of Bristol (15 kV, 15 nA, 15–30 s counting time). Fe metal, Ni metal, Cu metal, adularia, albite, periclase, olivine, spinel and FeS_2 were employed as standards. A defocused beam (usually 15 μm) was used to analyse both quenched silicate melt and quenched Fe alloys. Experiments with different beam sizes showed that 15–25 μm gave best averaging of compositions. The PAP correction procedure was used. Oxygen was analysed using Fe_2O_3 as the oxygen standard with beam conditions of 10 kV and 20 nA and a 5 μm beam. For experiments that contained a suite of high field strength trace

Table 2b
Experimental conditions of piston cylinder and multianvil partitioning experiments between silicate melt and Fe–sulphide liquid

Run No.	T	P	Time	Starting materials		Remarks	K/Na content in quenched liquid Fe–sulphide alloy
	(°C)	(GPa)	(min)	Fe alloy[a]	Silicate		
13	1600	2.5	65	$FeS_{82}Fe_{18}$	Sil		2.50 (1.4)/0.88 (0.40)
15	1600	2.5	60	FeS	Sil		1.17 (0.33)/1.13 (0.43)
17	1600	2.5	70	FeS	K-Sil+		0.63 (0.27)
21	1600	2.5	75	FeS	K-Sil+	Qtz. capsule	0.045 (0.019)
22	1600	2.5	60	FeS	K-Sil+	+Al_2O_3 (11 wt%)	1.62 (0.35)
23	1600	2.5	60	FeS	K-Sil+	+Si (1 wt%)	0.059 (0.005)
24	1600	2.5	60	$FeS_{80}FeSi_{20}$	K-Sil+	Qtz. capsule	Below D.L.
25	1600	2.5	60	$FeS_{90}FeSi_{10}$	K-Sil+	Qtz. capsule	Below D.L.
26	1600	2.5	40	$FeS_{75}FeO_{25}$	Sil	Qtz. capsule	0.029 (0.015)/0.054 (0.04)
27	1750	2.5	30	FeS	Sil		1.99 (0.76)/14.5 (2.9)
28	1750	2.5	30	$FeS_{75}FeO_{25}$	Sil	Qtz. capsule	Below D.L.
29	1500	2.5	70	FeS	Sil		0.89 (0.28)/2.97 (1.5)
30	1500	2.5	65	$FeS_{75}FeO_{25}$	Sil	Qtz. capsule	0.023 (0.015)/0.042 (0.03)
35	1900	24	10	FeS	K-Sil+	[b]	0.033 (0.014)
37	1750	8	5	FeS	K-Sil		0.115 (0.07)

Unless otherwise stated, metal and silicate powders were mixed in a 1:1 weight ratio. Unless stated otherwise, MgO capsules were used. Qtz = Quartz; Below D.L. = below the detection limit. Sil = Na- and K-bearing starting material (Table 1); K-Sil = Na-free starting starting material (Table 1); SiO_2+Chld. = K- and Na-chloride-bearing starting material (Table 1).
[a] Subscripts give wt% of the respective component in the metal alloy.
[b] Original run number H1205 (Bayerisches Geoinstitut).

elements, analysis conditions were 20 kV and 20 nA with a 50 s counting time for trace elements. The experimental details and run conditions of the high-pressure experiments are summarised in Table 2.

3. Results and discussion

Microprobe analyses of the experimental products are listed in Table 3 and the respective K and Na distribution coefficients between sulphide liquid and silicate melt are presented in Table 4. Under the pressure and temperature conditions of the experiments, both the silicate and Fe alloy phases were molten. Usually the Fe alloy forms a sphere in the centre of the sample, surrounded by quenched silicate melt. K and Na partition strongly into the silicate phases (thus being lithophile) if equilibrated with S-free or S-poor liquid Fe metal at 2.5 GPa and moderate temperatures (1600–1700°C). In such experiments, the K and Na concentrations in the Fe, Fe–FeO, FeNi, Fe–FeSi or FeSi metal phases are below the detection limits of the electron microprobe (Table 2a) and $D^{metal/silicate}$ are thus close to 0. In experiments performed with FeS or S-rich Fe alloys, on the other hand, the alkali elements readily enter the Fe–sulphide liquid. For example, at fixed temperature and pressure of 1600°C and 2.5 GPa, values of D_K and D_{Na} vary between 0 and 2.4 (Table 4). Since these variations cannot be due to pressure and temperature changes, it is clear that either the bulk composition of the silicate melt and/or that of the Fe–sulphide phase, or variations in oxygen and sulphur fugacities exert profound influences on partitioning behaviour.

3.1. Compositional influences on K and Na partitioning

A strong dependence of metal–silicate partition coefficients on the major element composition of the silicate melt has been reported for a number of elements (e.g. [17–19]). In order to illustrate this dependence, the melt composition is often represented as a single parameter, nbo/t, the ratio of non-bridging oxygen to tetrahedral cations (i.e. nbo/t = $[2\times N-4\times T]/T$; where N is the number of oxygen and T is the number of tetrahedrally coordinated cations). In our study the compositional effects were investigated by performing experiments separately in MgO and in SiO_2 capsules and in one experiment by varying the Al_2O_3 content of the melt. D_K and D_{Na} values (Table 4) as a function of nbo/t are shown, together with literature data, in Fig. 1A. D_K and D_{Na} values increase rapidly and approach unity with decreasing degree of polymerisation (increasing nbo/t). The data shown cover a broad range of P, T conditions, namely 1.5 –26 GPa and 1500–2600°C. Despite the much higher pressures and temperatures, the results of Ito [13] (26 GPa, 2600°C) and Ohtani et al. [11,14] (4–6 GPa, 1525–2585°C and 20 GPa, 2500°C respectively) on potassium partitioning agree well with the present data (mostly 2.5 GPa, 1500–1750°C). The main apparent discrepancy is the systematically lower (~one order of magnitude) D_K -values obtained by Chabot and Drake [10] (1.5 GPa, 1900°C). These are probably related to the use of graphite (instead of oxide) capsules. This supposition is more readily appreciated by examination of Fig. 1B where D_K and D_{Na} values are shown as a function of Si+Al content of the silicate melt. Shaded areas indicate results for different capsule materials and show a trend of decreasing D_K and D_{Na} values from MgO to SiO_2 to Al_2O_3 capsules. This trend correlates with increasing Si+Al and with decreasing nbo/t of the silicate melt. The results of experiments performed by Chabot and Drake [10] in graphite capsules exhibit a parallel trend shifted by about 1 log unit to lower D values. Since C is virtually insoluble in silicate melts under strongly reducing conditions, the effect illustrated in Fig. 1 must be due either to the presence of C (1 wt% or more) in the Fe–S alloys or to the effect of C on the oxygen fugacity of the experiment. As will be shown later, the latter cannot explain the lower D_K values, therefore the effect of alloy composition, which is described next, must be most important.

In virtually all our experiments in MgO capsules the product S-rich iron alloy quenched to a mixture of FeS and an oxygen and alkali-rich phase (Fig. 2), which, despite the presence of O,

Table 3
Electron microprobe analysis of run products (wt%)

Sulphide	#13	#15	#26	#27	#28	#29	#30	#37
Na	0.88 ± 0.40	1.13 ± 0.43	0.054 ± 0.040	14.54 ± 2.89	*	2.97 ± 1.50	0.042 ± 0.031	
K	2.50 ± 1.40	1.17 ± 0.33	0.029 ± 0.015	1.99 ± 0.76	*	0.88 ± 0.28	0.023 ± 0.015	0.115 ± 0.07
Si	29.40 ± 3.36	31.41 ± 1.81	38.26 ± 0.39	27.13 ± 2.50	41.02 ± 0.59	32.39 ± 1.24	35.88 ± 1.34	33.79 ± 1.11
Mg	*	*	*	*	*	*	*	*
Ca	*	0.24 ± 0.10	*	0.17 ± 0.08	*	0.076 ± 0.04	*	*
Fe	59.79 ± 3.87	57.62 ± 2.69	62.22 ± 0.48	47.23 ± 3.69	59.85 ± 0.81	59.38 ± 2.40	64.81 ± 1.69	63.16 ± 1.07
Al	*	*	*	*	*	*	*	*
Si	*	*	*	*	*	*	*	*
Ni								*
O by diff.[a]	6.98 ± 3.91	8.34 ± 3.76		8.67 ± 3.87		4.09 ± 2.40		2.85 ± 1.51
Silicate	#13	#15	#26	#27	#28	#29	#30	#37
Na	1.19 ± 0.51	4.24 ± 0.35	2.27 ± 0.04	2.90 ± 1.33	1.30 ± 0.06	4.78 ± 1.46	2.05 ± 0.09	
K	1.03 ± 0.46	3.58 ± 0.22	2.34 ± 0.04	2.78 ± 1.22	1.66 ± 0.04	4.65 ± 1.20	2.32 ± 0.04	1.182 ± 0.64
S	0.38 ± 0.16	0.56 ± 0.11	0.28 ± 0.03	0.55 ± 0.30	0.30 ± 0.03	0.39 ± 0.09	0.22 ± 0.06	0.217 ± 0.26
Mg	25.44 ± 2.28	12.30 ± 1.64	4.35 ± 0.08	21.55 ± 4.58	4.29 ± 0.11	12.73 ± 5.50	5.49 ± 0.06	22.015 ± 3.47
Ca	2.51 ± 0.97	7.61 ± 0.67	2.24 ± 0.05	4.64 ± 1.62	2.07 ± 0.05	5.60 ± 1.60	2.41 ± 0.04	6.510 ± 2.64
Fe	2.55 ± 0.47	3.63 ± 0.17	9.68 ± 0.21	2.96 ± 0.47	7.15 ± 0.20	3.90 ± 0.19	9.35 ± 0.20	2.422 ± 0.46
Al	1.14 ± 0.54	4.42 ± 0.26	1.64 ± 0.03	4.39 ± 1.46	2.56 ± 0.51	3.78 ± 0.83	1.58 ± 0.03	3.213 ± 1.32
Si	17.04 ± 1.28	21.20 ± 0.20	31.18 ± 0.22	17.75 ± 0.78	32.70 ± 0.47	20.75 ± 0.50	30.36 ± 0.19	16.026 ± 0.82
O	40.10 ± 3.17	43.30 ± 0.55	46.02 ± 0.32	42.46 ± 1.35	47.97 ± 0.36	43.42 ± 0.58	46.22 ± 0.39	39.816 ± 1.65

Sulphide	#17	#21	#22	#23	#24	#25	#35
Na							
K	0.629 ± 0.27	0.045 ± 0.02	1.616 ± 0.35	0.059 ± 0.01	*	*	0.033 ± 0.01
S	34.032 ± 1.04	35.629 ± 0.58	34.103 ± 1.59	24.341 ± 0.58	32.643 ± 2.00	30.997 ± 1.86	32.793 ± 0.45
Mg	*	0.100 ± 0.08	*	*	0.172 ± 0.05	*	*
Ca	0.194 ± 0.13	0.349 ± 0.13	0.131 ± 0.07	0.108 ± 0.01	*	0.194 ± 0.22	*
Fe	61.619 ± 1.14	62.566 ± 0.53	57.475 ± 1.83	73.796 ± 0.77	67.227 ± 1.82	68.810 ± 1.87	60.309 ± 0.72
Al	*	*	*	*	*	*	*
Si	*	*	0.295 ± 0.21	*	*	*	*
Zr	*	*	*	*	0.047 ± 0.03	*	*
Nb	*	*	*	0.551 ± 0.01	0.153 ± 0.06	*	*
Th	*	*	*	*	*	*	*
U	*	*	*	*	0.098 ± 0.04	*	*
Lu	*	*	*	*	*	*	*
Hf	*	*	*	*	*	*	*
Zn	0.068 ± 0.03	0.068 ± 0.03	*	0.098 ± 0.01	0.135 ± 0.03	0.070 ± 0.02	0.659 ± 0.04
Pb	0.072 ± 0.08	0.070 ± 0.08	0.082 ± 0.09	0.050 ± 0.04	0.088 ± 0.08	0.108 ± 0.08	*
Sm	*	*	*	*	*	*	*
Nd	*	*	*	*	*	*	*
O by diff.[a]	3.137 ± 0.96	0.947 ± 0.55	6.081 ± 2.65	0.788 ± 0.66			6.062 ± 0.81
Silicate	#17	#21	#22	#23	#24	#25	#35
Na							
K	5.092 ± 0.65	3.226 ± 0.03	4.670 ± 0.85	4.863 ± 0.25	3.866 ± 0.04	3.663 ± 0.05	0.381 ± 0.19
S	0.766 ± 0.28	1.357 ± 0.05	0.762 ± 0.35	2.042 ± 0.16	6.156 ± 0.09	3.613 ± 0.14	0.071 ± 0.14
Mg	12.359 ± 3.38	7.037 ± 0.04	13.597 ± 3.73	13.546 ± 0.88	9.279 ± 0.12	8.753 ± 0.07	15.891 ± 3.10
Ca	7.617 ± 1.51	4.205 ± 0.03	9.244 ± 2.28	6.877 ± 0.62	4.807 ± 0.04	5.108 ± 0.05	7.885 ± 3.60
Fe	1.366 ± 0.40	0.572 ± 0.04	1.988 ± 0.51	0.313 ± 0.04	0.288 ± 0.05	0.306 ± 0.04	2.296 ± 0.75
Al	7.324 ± 0.88	2.190 ± 0.02	9.043 ± 2.82	4.440 ± 0.18	2.682 ± 0.03	2.458 ± 0.05	2.102 ± 1.43
Si	20.652 ± 0.34	33.392 ± 0.13	18.215 ± 1.40	23.720 ± 0.14	30.224 ± 0.23	30.695 ± 0.23	24.188 ± 1.43
Zr	0.118 ± 0.04	0.052 ± 0.02	*	0.115 ± 0.02	0.052 ± 0.02	*	*

Table 3 (*Continued*)

Silicate	#17	#21	#22	#23	#24	#25	#35
Nb	0.083 ± 0.03	*	*	*	*	*	*
Th	0.120 ± 0.03	0.047 ± 0.02	*	0.125 ± 0.02	0.062 ± 0.03	0.051 ± 0.02	*
U	0.105 ± 0.03	0.048 ± 0.02	*	0.101 ± 0.02	*	*	*
Lu	0.118 ± 0.04	0.061 ± 0.03	*	0.110 ± 0.02	0.075 ± 0.03	0.052 ± 0.03	*
Hf	0.128 ± 0.04	0.057 ± 0.03	*	0.121 ± 0.03	0.061 ± 0.03	0.060 ± 0.03	*
Zn	*	*	*	*	*	*	*
Pb	*	*	*	0.066 ± 0.06	*	*	*
Sm	0.099 ± 0.03	0.051 ± 0.02	*	0.079 ± 0.03	0.046 ± 0.03	*	*
Nd	0.072 ± 0.03	0.030 ± 0.02	*	0.045 ± 0.02	*	*	*
O	44.037 ± 0.71	47.757 ± 0.21	42.430 ± 0.73	43.500 ± 0.30	42.437 ± 0.42	45.235 ± 0.38	43.943 ± 1.19

* = below detection limit; empty field = element not present in starting material.

[a] Oxygen contents by difference were calculated considering full analysis (i.e. including *contents which have been omitted here).

may be related in composition to djerfisherite, $K_6Na(Cu,Fe,Ni)_{25}S_{26}Cl$, a mineral occurring in enstatite chondrite meteorites (e.g. [20,21]). No other alkali–Fe–sulphide simultaneously carrying Na and K is presently known. Missing Cu, Ni and Cl compared to natural djerfisherite are due to Cu-, Ni- and Cl-free starting materials. However, a Cl-free analogue of djerfisherite was recently reported [22]. Also, Fe/alkali and S/alkali ratios of the experimental run products are similar to those of djerfisherite. Furthermore, the intergrown alkali-rich phases are much softer than the surrounding Fe–sulphide phases and, as previously reported for djerfisherite [20] can only be polished with difficulty. Apparent chalcophile behaviour of Na has also been observed in shock-melted meteorites by Leroux et al. [23]. In addition, these authors suggest that significant Mg and Si in quenched sulphides may be due to the incorporation of silicate nanoparticles during the shock event. Lack of detectable Mg and Si in virtually all experimentally produced sulphide liquids (Table 3) shows that silicate nanoparticles are not important contaminants in our experiments. Because Fe–sulphide and alkali-rich phases are intergrown at a very fine scale, the quenched iron–sulphide liquids were usually analysed with a beam defocussed to 15–25 μm diameter. If substantial Na is present in the starting material, the interstitial alkali- and oxygen-rich djerfisherite-

Table 4
Experimental results

Run No.	P (GPa)	T (°C)	nbo/t	D_K	D_{Na}	O by diff.	$X_{anions}/X_{cations}$
13	2.5	1600	3.73	2.434(±1.7)	0.739(±0.46)	6.98	1.1536
15	2.5	1600	1.89	0.327(±0.09)	0.266(±0.103)	8.34	1.3514
17	2.5	1600	1.467	0.124(±0.065)		3.14	1.1239
21	2.5	1600	0.7	0.014(±0.006)		0.95	1.0540
22	2.5	1600	1.391	0.346(±0.098)		6.08	1.3554
23	2.5	1600	1.39	0.012(±0.0013)		0.79	0.6216
24	2.5	1600	0.513	Below D.L.	Below D.L.	0	1.1800
25	2.5	1600	0.776	Below D.L.	Below D.L.	0	1.274
26	2.5	1600	0.914	0.012(±0.006)	0.024(±0.017)	0	1.0674
27	2.5	1750	2.672	0.719(±0.42)	5.011(±2.5)	8.67	0.9106
28	2.5	1750	0.764	Below D.L.	Below D.L.	0	1.1916
29	2.5	1500	2.192	0.190(±0.077)	0.622(±0.37)	4.09	1.0458
30	2.5	1500	1.0711	0.01(±0.006)	0.02(±0.015)	0	0.9622
35	24	1900	1.846	0.087(±0.057)		6.17	1.3031
37	8	1750	3.215	0.097(±0.079)		2.85	1.0867

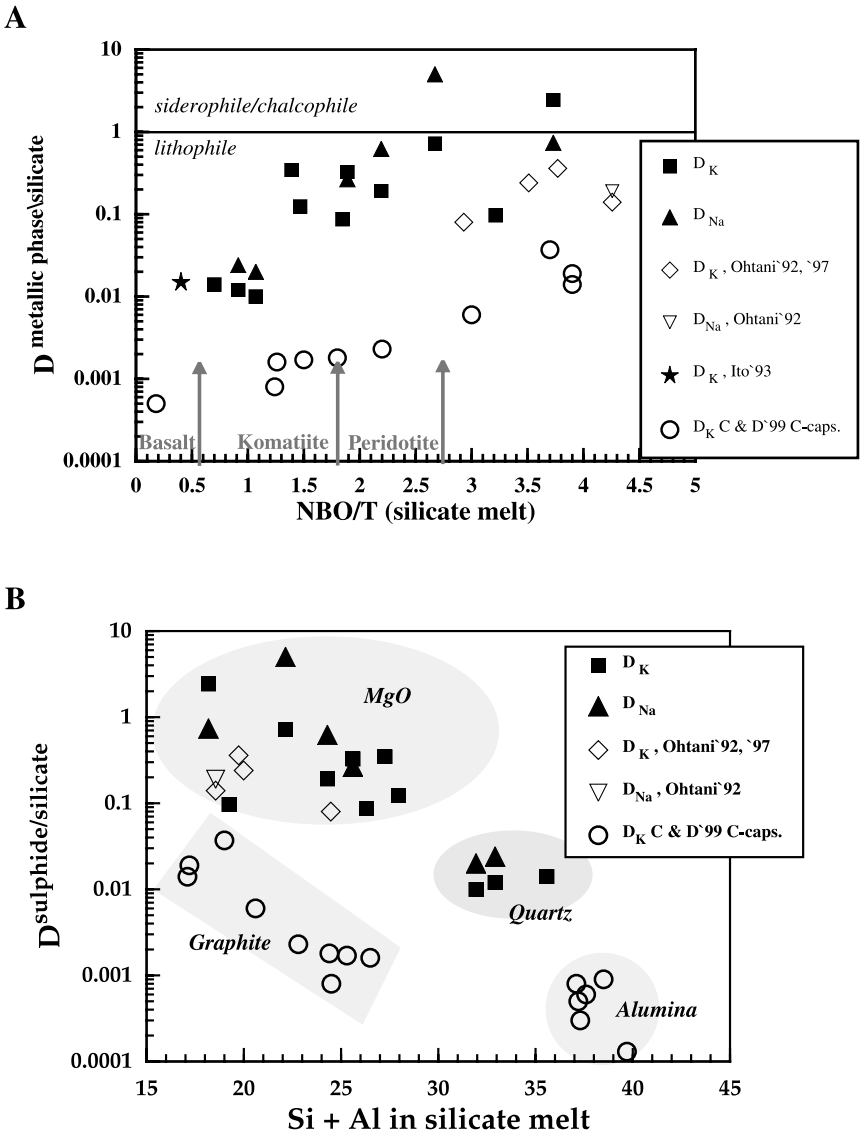

Fig. 1. (A) K and Na distribution coefficients between Fe alloys and silicate melt as a function of nbo/t (nbo/t = non-bridging oxygen atoms/tetrahedrally coordinated cations in silicate melt). Data of Ito [13] (26 GPa, 2600°C) and Ohtani et al. [11,14] (4–6 GPa, 1525–2585°C and 20 GPa, 2500°C respectively) agree well with the present results. The systematically lower D_K values of Chabot and Drake [10] (1.5 GPa, 1900°C) can be related to the presence of carbon. (C-free experiments from [10] are not shown because of 0 or negative nbo/t values.) Nbo/t values for rock compositions are given for comparison along the *x*-axis. The horizontal line at $D = 1$ indicates the change from lithophile to chalcophile behaviour of the alkali elements. (B) D_K and D_{Na} values as a function of Si+Al content of the silicate melt. The shaded areas indicate different capsule materials. *D* values decrease as a function of increasing Si+Al content of the silicate melt. Carbon bearing experiments are displaced to lower *D* values.

like phase reacts within hours with the atmosphere, even if stored in an evacuated desiccator. Sample preparation and microprobe analysis of Na-bearing products were therefore performed within the shortest time possible, usually a day. Nevertheless, results for Na-bearing charges usually have large uncertainties. Due to this tendency to decomposition, most experiments were per-

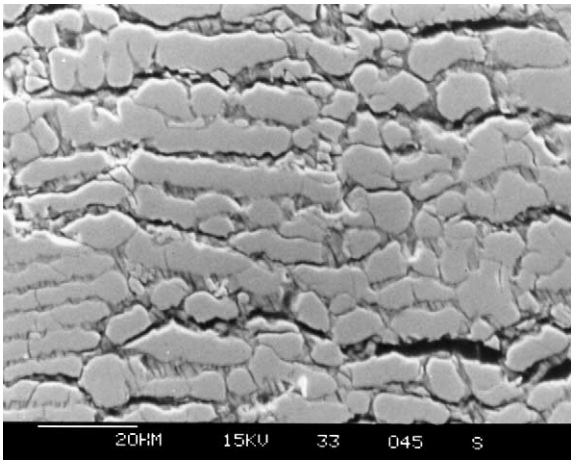

Fig. 2. Quench texture of the Fe–sulphide liquid after the experiment. The Fe–sulphide liquid quenches into an FeS compound and interstitial K-, Na- and O-rich Fe–sulphide phases, similar to Djerfisherite in composition.

formed with Na-free starting materials. Products from the latter usually show less distinct quench textures.

Because microprobe analysis of the Fe–sulphide liquids often had low totals, the presence of oxygen in these alloys was suspected and confirmed by energy dispersive and quantitative microprobe analysis. Despite our determination of up to 7% O, the microprobe totals are still below 100 (up to several wt%), implying that the measured O content is lower than the true value. The O measurements have considerable uncertainty, however, because of the very high absorption of the K_α radiation of oxygen by the matrix, in particular by S, which results in poorly constrained correction factors, and because of the heterogeneous nature of the intergrowths. Using difference of total from 100% as an alternative indication of oxygen content (Fig. 3A) generally gives higher O concentrations. The two methods generally agree within uncertainty, however. Although below we use the difference method, this choice does not substantively affect the results or conclusions of this study. Substitution of O for S in sulphide melts has also been reported in a number of experimental studies on the Fe–S–O system at 1 bar (e.g. [24,25]) as well as in high-pressure element partitioning (e.g. [26]). The two important compositional parameters are the ratio ([O+S]/Fe) and the ratio of O/S. The latter is illustrated in Fig. 3B.

Fig. 4A shows that the distribution coefficient of K apparently increases with increasing anion/cation ([O+S]/[Fe+Na+K]) ratio of the Fe–sulphide liquid. There is also some indication, illustrated by the sketched lines in Fig. 4A, that effects of both anion/cation in the Fe–sulphide liquid

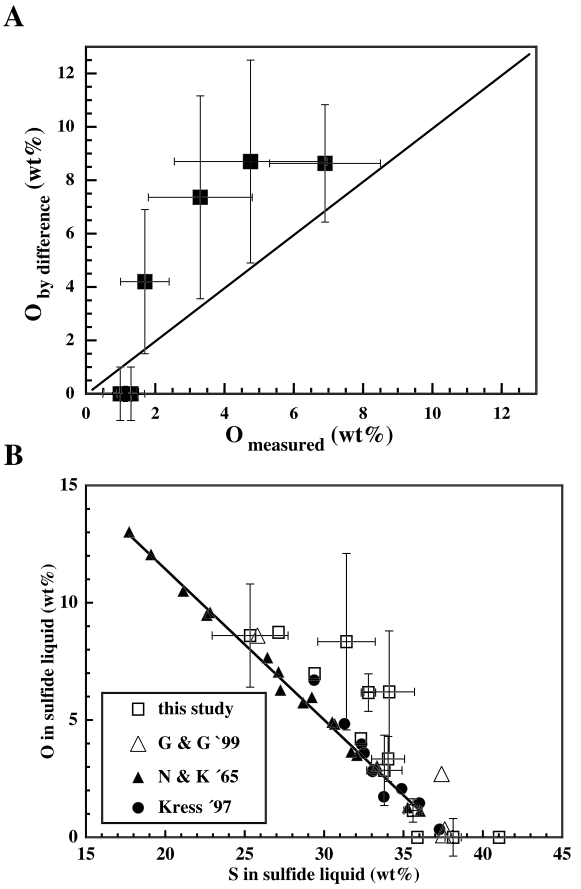

Fig. 3. (A) Oxygen contents estimated by analysis total as a function of measured oxygen contents in selected samples. The estimated O values are generally higher than the measured O contents as indicated by the deviation from the 1:1 reference line. However, within uncertainty the two methods agree. (B) Oxygen content versus sulphur content of Fe–sulphide liquids in 1 bar and high-pressure experiments. The regression line describes the 1200°C data of Nagamori et al. [24]. The O contents determined by total deficiency generally follow the trend defined by literature data. Error bars are shown for representative samples.

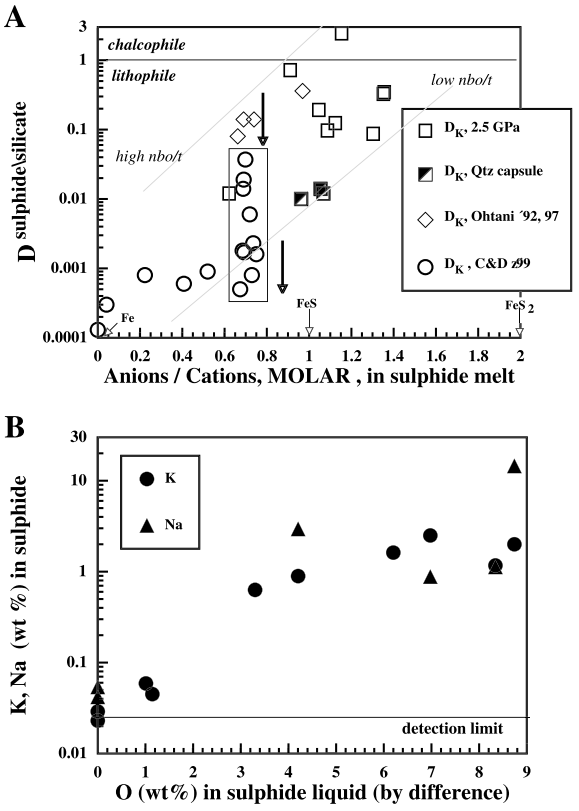

Fig. 4. (A) K distribution coefficients as a function of anion/cation ratio ([O+S]/[Fe+K+Na]) of sulphide melt. D_K increases with increasing anion content of the sulphide melt. Various Fe compounds are indicated on the *x*-axis. The arrows indicate the shift of the C-bearing experiments of Chabot and Drake [10] to lower *D* values. Diagonal broken lines indicate low (~0) and high (~4) nbo/t values of the experimental results. (B) K and Na contents of sulphide melts increase with increasing O content of the sulphide melt.

and nbo/t in the silicate melt are significant. The highest D_K values (close to unity) are obtained in experiments with high anion/cation ratio of the Fe–sulphide liquid, which also corresponds to high oxygen contents (see Fig. 4B). It should be noted that those experimental products of Chabot and Drake [10] that have the highest values of D_K have Fe–sulphide alloys with low analysis totals (2.2–5.1 wt% deficient). Fe–sulphide liquids in these experiments may also, therefore, contain some oxygen.

Examination of Figs. 1 and 4 implies, empirically, that the important compositional controls on D_K are either nbo/t of the silicate melt *or* anion/cation ratio of the Fe–sulphide liquid *or* both. Some idea of the relative influences of silicate melt composition and anion/cation ratio in the Fe–sulphide liquid on K partitioning was obtained by fitting a small data set of eight experiments at constant *P*, *T* conditions (2.5 GPa, 1600°C) to the equation:

$$\ln D_K = a_1 + a_2 \times \mathrm{nbo/t} + a_3 \times (X_{\mathrm{anions}}/X_{\mathrm{cations}}) \quad (1)$$

yielding

$$\ln D_K = \underset{\pm 1.03}{-9.63} + \underset{\pm 0.23}{1.52} \times \mathrm{nbo/t} + \underset{\pm 0.89}{4.39} \times (X_{\mathrm{anions}}/X_{\mathrm{cations}})$$

Eq. 1 describes the experiments with an average deviation of 22% in ln*D*. The nbo/t parameter is in reasonable agreement with that derived by Chabot and Drake [10] and the equation implies that both silicate and sulphide melt compositions affect partitioning. Since, however, the fugacities of oxygen and sulphur have not yet been considered it is clear that, if possible, the results must be placed in a thermodynamic framework in order to improve our understanding of the important effects.

Kress [27] presented a thermodynamic model for alloys in the system Fe–S–O which, although strictly only applicable at 1 bar, provides a means of calculating, from alloy composition and temperature, the activities of oxygen, sulphur and iron in the system. The model contains 16 fit parameters and can only be solved numerically. In order to apply the model to the calculation of activities in our sulphide alloys the calculator at the web-site [28] was used. This model was applied to the present data to investigate the influence of these thermodynamic parameters.

Fig. 5A shows the partitioning of K plotted as a function of log fO_2 for those experiments in which the alloy content of oxygen is greater than zero, so that Kress' [27] model may be applied. As noted above, the effect of pressure has been ignored and, for those experiments performed at temperature above the maximum at

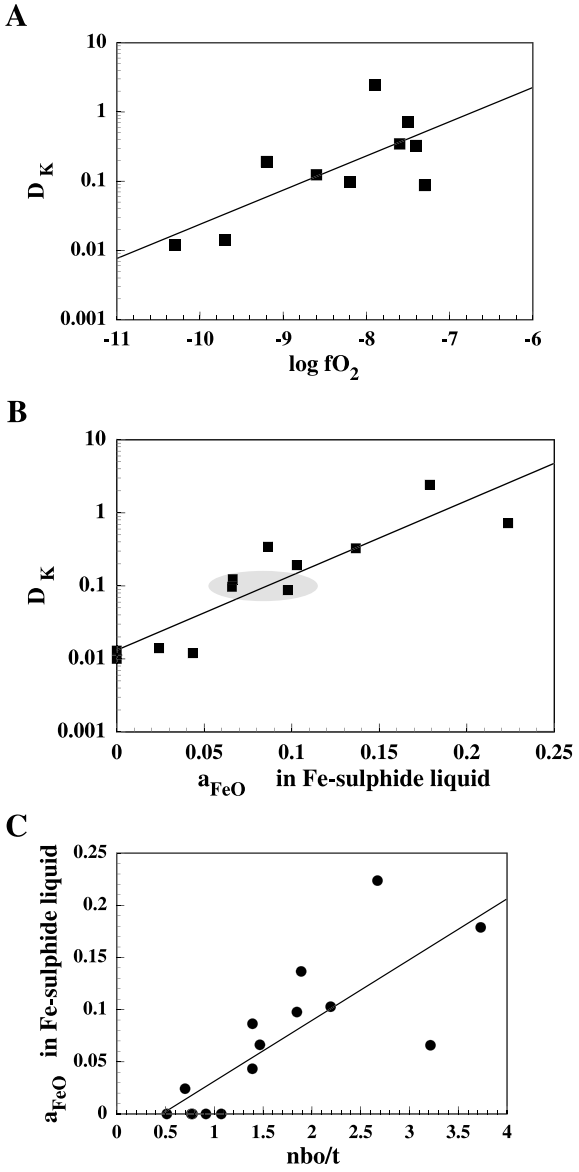

Fig. 5. (A) Distribution coefficients of K (Fe–sulphide liquid/silicate melt) as a function of oxygen fugacity calculated according to the model of Kress [27]. Note that positive correlation implies an impossibly high oxidation state (>+1) for K in the Fe–sulphide liquid. (B) Fe–sulphide liquid–silicate melt distribution coefficients for K as a function of the a_{FeO} of the Fe–sulphide liquids (from [27]) showing a strong correlation. The shaded field denotes the *P*-dependent experiments (see text and Fig. 7). (C) a_{FeO} of the Fe–sulphide liquid (from [27]) as a function of nbo/t of the silicate melt.

which the model is valid, 1700°C, the calculation was performed at the latter temperature. As can be seen, there is a rough positive correlation between D_K and oxygen fugacity, implying that the oxidation state of potassium is *larger* in the Fe–sulphide phase than in the silicate. Since the oxidation state of K in the silicate is the greatest possible, +1, the observed correlation cannot be due to a redox equilibrium involving K. Because bulk alkali and oxygen contents of the Fe–sulphide alloy are definitely correlated (Fig. 4B), a more likely explanation is that the oxygen content of the Fe–sulphide liquid, thermodynamically expressed as the activity of FeO, is the parameter controlling D_K. K and O occur together with Fe in the soft quench phase implying a strong chemical affinity between the three elements in sulphide melts. Fig. 5B shows that the correlation between D_K and a_{FeO} is good, a logical result given the textural and chemical data described above. Assuming that the model of Kress [27] provides a reasonable representation of a_{FeO} it is of interest to consider the reasons for variation of a_{FeO} in experiments that start with similar bulk composition. Given the large variation in a_{FeO} (Fig. 5B) the most likely explanation is that it is principally due to changes in oxide ion O^{2-} activity in the silicate melt (e.g. [29]). This may be qualitatively seen in Fig. 5C, a plot of FeO activity in Fe–sulphide liquid against nbo/t where the latter is a measure of O^{2-} in the silicate melt.

If we assume that, instead of the parameters in Eq. 1, the activity of FeO in the Fe–sulphide liquid is the major factor controlling K partitioning, then the eight experiments at 2.5 GPa and 1600°C fit the following equation with an average deviation of 32% in ln*D*.

$$\ln D_K = \begin{matrix} -4.70 + 30.7 \times a_{FeO}^{Fe-sulphide} \\ \pm 0.48 \ \pm 5.02 \end{matrix} \quad (2)$$

The fit is slightly better, however (average deviation of 30% in ln*D*), if the anion/cation ratio of the sulphide liquid is also considered:

$$\ln D_K = \underset{\pm 1.23}{-6.80} + \underset{\pm 4.7}{26.77 \times a_{FeO}^{Fe-sulphide}} + \underset{\pm 1.2}{2.18 \times (X_{anions}/X_{cations})} \quad (3)$$

Considering uncertainties of estimated a_{FeO} with the 1 bar model of Kress, the regressions imply that the activity of FeO in Fe–sulphide liquid is probably the most important factor controlling the partitioning of K. However, both Eqs. 1 and 3 describe the experimental data equally well.

3.2. Influence of temperature on D_K and D_{Na}

Fig. 6 shows a set of isobaric experiments (2.5 GPa) and temperatures of 1500–1750°C. The alkali elements partition more strongly into the Fe–sulphide liquid with increasing temperature. Considering the less well-constrained trend for Na compared to K, the distribution coefficients approach unity at around 1700–1800°C. Although anion contents and anion/cation ratios of the Fe–sulphide liquid as well as nbo/t in the silicate melt are almost constant for this set of experiments, the a_{FeO} and the O contents of the Fe–sulphide liquids increase with increasing temperature (Fig. 6). Increasing O solubility as a function of temperature is also reported for S-free liquid Fe alloys [30,31]. The observed increase in alkali distribution coefficients with increasing temperature in Fig. 6 may thus be predominantly ascribed to compositional effects, i.e. enhanced O content with increasing temperature.

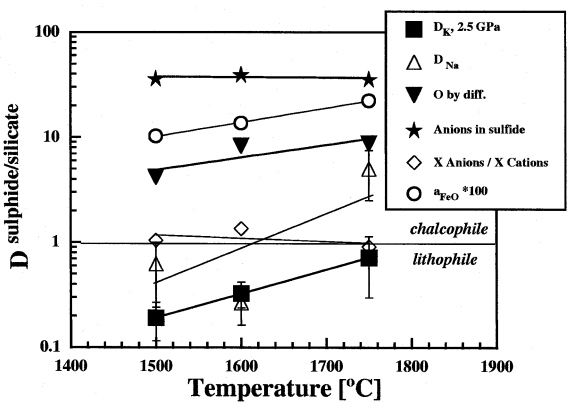

Fig. 6. Fe–sulphide liquid–silicate melt distribution coefficients of K and Na as a function of temperature at constant pressure (2.5 GPa) showing increasingly chalcophile behaviour of the alkali elements with increasing temperature. The O and anion contents (S+O) of the Fe–sulphide liquids, their anion/cation ratios and their a_{FeO} values are also shown. The horizontal line indicates $D = 1$, i.e. the change from lithophile to chalcophile behaviour of the alkali elements. The other lines are regression lines.

3.3. Influence of pressure on D_K

First results on the effect of pressure on the partitioning of K are shown in Fig. 7A. Because in these experiments pressure, temperature and O contents of the sulphide melts all increased, the observed effects on K partitioning cannot be solely ascribed to the influence of pressure. According to the results discussed above, D_K and O contents of the Fe–sulphide liquids increase with increasing temperature. In this pressure-dependent set of experiments however, the distribution coefficients decrease slightly, despite increasing temperature and O content of the Fe–sulphide liquid. It appears therefore that, at fixed temperature and O content, D_K decreases with increasing pressure.

In order to describe the magnitude of the negative pressure effect on the distribution coefficients of K, two sets of experiments (from Figs. 6 and 7A) are compared in Fig. 7B. All experiments, except those labelled, were performed at 2.5 GPa. In the case of no pressure effect on K partitioning, the regression line for the *P*-dependent set of experiments would be similar or parallel to the isobaric set of experiments (broken line). This is not the case and therefore, comparison of the regression lines (isobaric and *P*-dependent) enables us to estimate the negative pressure effect on D_K to be about almost one order of magnitude at 25 GPa and 1900°C as indicated by the arrow.

3.4. Siderophile/chalcophile character of light elements

Even at very low pressures and temperatures S is completely miscible in Fe alloys so may be considered siderophile under all conditions relevant to core formation. In the cases of oxygen and silicon, however, siderophile and/or chalcophile

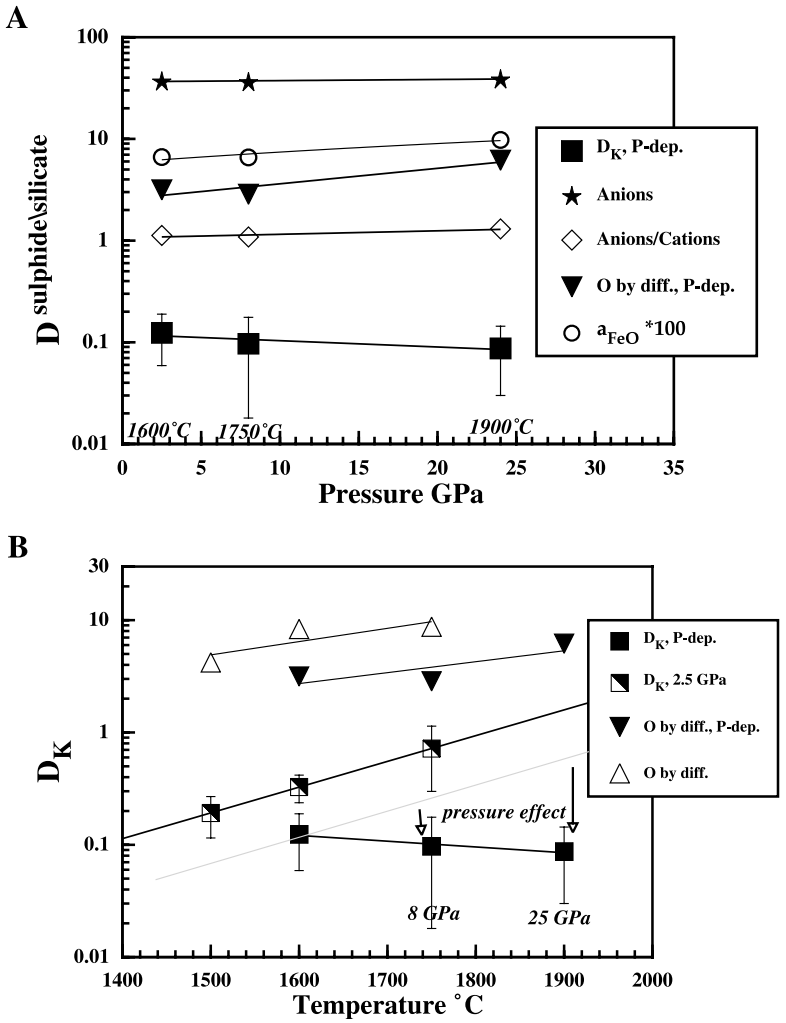

Fig. 7. (A) Distribution coefficients of K as a function of pressure. Oxygen contents, anion contents, anion/cation ratios and a_{FeO} values of the Fe–sulphide liquid are also shown. The temperature of the experiments was also increased (see labels). Despite increasing temperature, the D_K values decrease slightly. (B) K distribution coefficients and O contents in Fe–sulphide liquid as a function of temperature. An isobaric (2.5 GPa) and a pressure-dependent set of experiments (see labels) are shown. The arrows indicate the effect of pressure on D_K comparing the 2.5 GPa data set with a pressure-dependent set of experiments.

behaviour is not so obvious since O and Si solubilities in Fe alloys depend strongly on pressure, temperature and oxygen fugacity. In the present study, significant amounts of oxygen (up to 8 wt%) enter the Fe–sulphide liquid together with the alkali metals. These amounts are distinctly higher, about an order of magnitude, than previously reported O solubility in S-free liquid metal [16,30,31]. O solubility in Fe alloys is therefore greatly enhanced by the presence of sulphur.

4. Summary and conclusions

Neither K nor Na is truly siderophile under the conditions we have investigated (i.e. in S-free and S-poor experiments). For equilibrium between S-rich Fe–sulphide liquids and silicate melt, however, the D values of K and Na approach unity (thus indicating chalcophile behaviour) with increasing oxygen content of the sulphide melt. In other words, according to the experimental re-

sults, only S-rich Fe–sulphide liquids dissolve significant K and Na. Moreover, different capsule materials strongly influence the alkali distribution coefficients due to their effects on silicate melt composition (reaction between capsule material and silicate melt). The combination of these two effects helps explain the large range of published D_K values (four orders of magnitude). The results also indicate that a segregating Fe–sulphide liquid would not only transport significant amounts of alkali metals into Earth's core but probably also oxygen. Thus S and O comprise an element combination which may contribute significantly to the light element content of the Earth's core.

In the context of core formation processes, our results indicate that, at pressure and temperature conditions that are relevant to the segregation of core-forming material (i.e. a magma ocean) some K and Na may be sequestered into the core with S-rich Fe–sulphide liquids. Due to the small and not very well constrained set of data for Na, only the K results will be further discussed in the following. With a known mantle concentration (e.g. $\sim$240 ppm for K [5]) and assuming that $D = c_{metal}/c_{silicate}$ equals c_{core}/c_{mantle} the core concentration of a given element can be calculated: $c_{core} = D \times c_{mantle}$. Assuming an O-rich Fe–sulphide liquid ($X_{anion} = 0.5$–0.6) and a peridotite magma composition (nbo/t = 2.8), the latter corresponding to $a_{FeO} \approx 0.15$, D_K values above unity at low pressure and temperature (e.g. 2.5 GPa, 1800°C) can account for several hundred ppm K in segregating S-rich Fe–sulphide liquid. This is an important result with respect to small planetary bodies such as Mars or the Aubrite Parent Body. In particular for Mars, with its small size and the plausible high core content of S, significant amounts of K in its core seem likely. For the Earth, however, recent studies suggest much deeper and hotter magma ocean scenarios for core segregation [32–34]. Although pressure reduces Fe–sulphide liquid–silicate melt distribution coefficients of K, high temperature has, through enhanced O solubility, the opposite effect. Extrapolation of the D_K from the current experiments to P, T conditions that have been suggested for core formation, i.e. $\sim$25 GPa, 2000°C [33] and $\sim$35 GPa, $>$3300°C [34], yield D_K values on the order of 0.2 to 1.3 respectively (at $X_{anion} = 0.55$, $a_{FeO} = 0.15$, or at $X_{anion} = 0.55$ and nbo/t = 2.8). Note, however, that due to the small data set and large uncertainties on D_K values, these extrapolated D values are poorly constrained. If, for illustration, we take the upper limits of the estimated D values ($D_K = 1.3$) and of the S content in the core (10 wt%; corresponding to $\sim$1/3 of the S content in the experimental Fe–sulphide liquid) then, given a mantle concentration of 240 ppm K [5], about 100 ppm K in the core is conceivable. Note that 10 wt% S is thought to be the required amount to account for the entire density deficit of the Earth's core (summarized in [35]). Therefore it is assumed that the segregating core is approximately 1/3 Fe–sulphide and 2/3 liquid Fe (essentially K-free). A K content of 100 ppm is much higher than previous estimates and could provide up to 7% of the energy required for the core dynamo [7]. According to the present results, a maximum K content in the core would be achieved if core formation involved an O-rich Fe–sulphide liquid with very high anion content (e.g. X_{anion} 0.59, $a_{FeO} = 0.18$). In this (rather unlikely) case, the same conditions would result in even higher D_K values, i.e. 0.5 to 3.5, the latter yielding a maximum of $\sim$250 ppm K in an S-rich (10 wt%) core formed from a mixture of Fe–sulphide and Fe–metal liquids. Given a specific elemental heat production of 3.45×10^{-9} W/kg [36], this K content would currently provide $\sim$20% of the energy required to power the core dynamo ($\sim 10^{13}$ W, maximum estimate of [7]). The initial heat production (i.e. after core formation), however, would have been much higher than 10^{13} W.

With respect to the question of whether or not there is K present in the Earth's core and the cores of other planetary bodies, it should be kept in mind that K can enter core-forming segregating Fe alloys only under very restricted conditions. In particular, the presence of an oxygen- and sulphur-rich Fe–sulphide liquid at some point during core formation is required in order to dissolve significant amounts of K into the segregating Fe alloy. Even if such conditions prevailed during core formation, ^{40}K decay probably provides no more than 20% of the energy required to power the geodynamo. If the potential amount of

S in the core is far less (e.g. <2 wt% [37]), the K content in the core must be much smaller. If S is absent from the core, the K content in the core is almost certainly negligible.

Acknowledgements

Advice and assistance by Stuart Kearns with microprobe work and of Fred Wheeler and workshop colleagues is highly appreciated. Comments and suggestions by F. Guyot and two anonymous reviewers improved the manuscript. We acknowledge the award of TMR Marie Curie Fellowship ERBBFMBICT 972416 (to C.G.) and NERC Grant GR3/11535 and a Max Planck Research Award (to B.W.). The 24 GPa experiment was funded by the EU 'Human Capital and Mobility – Access to Large Scale Facilities' programme (Contract No. ERBCHGECT940053).*[BARD]*

References

[1] K. Lodders, Alkali elements in the Earth's core: Evidence from enstatite meteorites, Meteoritics 30 (1995) 93–101.
[2] M.S.T. Bukowinski, The effect of pressure on the physics and chemistry of potassium, Geophys. Res. Lett. 3 (1976) 491–503.
[3] M.S.T. Bukowinski, L. Knopoff, Physics and chemistry of iron and potassium at lower-mantle and core pressure, in: M.H. Manghnani, S. Akimoto (Eds.), High Pressure Research, Applications in Geophysics, 1977, pp. 367–387.
[4] L.J. Parker, T. Atou, J.V. Badding, Transition element-like chemistry for potassium under pressure, Science 273 (1996) 95–97.
[5] W.F. McDonough, S.-s. Sun, The composition of the Earth, Chem. Geol. 120 (1995) 223–253.
[6] C.A. Stein, Heat flow of the earth, in: T.H. Ahrens (Ed.), Global Earth Physics, A Handbook of Physical Constants, AGU Reference Shelf 1, AGU, Washington, DC, 1995, pp. 144–158.
[7] D. Gubbins, T.G. Masters, J.A. Jacobs, Thermal evolution of the Earth's core, Geophys. J. R. Astron. Soc. 59 (1979) 57–99.
[8] J.A. Jacobs, The Earth's Core, Academic Press, London, 1987, 413 pp.
[9] M.T. Murrell, D.S. Burnett, Partitioning of K, U and Th between sulfide and silicate liquids implications for radioactive heating of planetary cores, J. Geophys. Res. B 91 (1986) 8126–8136.
[10] N.L. Chabot, M.J. Drake, Potassium solubility in metal: The effects of composition at 15 kbars and 1900°C on partitioning between iron alloys and silicate melts, Earth Planet. Sci. Lett. 172 (1999) 323–335.
[11] E. Ohtani, T. Kato, K. Onuma, E. Ito, Partitioning of elements between mantle and core materials and early differentiation of the Earth, in: Y. Syono, M.H. Manghnani (Eds.), High Pressure Research: Application to Earth and Planetary Science, Terrapub., Tokyo, 1992, pp. 341–349.
[12] E. Ohtani, H. Yurimoto, T. Segawa, T. Kato, Element partitioning between $MgSiO_3$ perovskite, magma and molten iron: Constraints on the earliest processes of the Earth-Moon system, in: T. Yukutake (Ed.), The Earth's Central part: Its Structure and Dynamics, Terra Scientific, Tokyo, 1995, pp. 287–300.
[13] E. Ito, K. Morooka, Dissolution of K in molten iron at high pressure and temperature, Geophys. Res. Lett. 20 (1993) 151651–151654.
[14] E. Ohtani, H. Yuriomoto, S. Seto, Element partitioning between metallic liquid, silicate liquid and lower-mantle minerals: implications for core formation of the Earth, Phys. Earth Planet. Inter. 100 (1997) 97–114.
[15] R.C. Liebermann, W. Wang, Characterization of Sample Environment in an Uniaxial Split-Sphere Apparatus, Terrapub., Tokyo, 1992.
[16] C.K. Gessmann, D.C. Rubie, The effect of temperature on the partitioning of Ni, Co, Mn, Cr and V at 9 GPa and constraints on formation of the Earth's core, Geochim. Cosmochim. Acta 62 (1998) 867–882.
[17] M.J. Walter, Y. Thibault, Partitioning of tungsten and molybdenum between metallic liquid and silicate melt, Science 270 (1995) 1186–1189.
[18] V.J. Hillgren, M.J. Drake, D.C. Rubie, High pressure and high temperature metal-silicate partitioning of siderophile elements: The importance of silicate liquid composition, Geochim. Cosmochim. Acta 60 (1996) 2257–2263.
[19] D. Jana, D. Walker, The influence of silicate melt composition on distribution of siderophile elements among metal and silicate liquids, Earth Planet. Sci. Lett. 150 (1997) 463–472.
[20] L.H. Fuchs, Alkali copper-iron sulfide: A new mineral from enstatite chondrites, Science 153 (1966) 166–167.
[21] A. El Goresy, H. Yabuki, K. Ehlers, D. Woolum, E. Pernicka, Quingzhen and Yamato-691: A tentative alphabet for the EH chondrites, in: NIPR Symposium on Antarctic Meteorites 1, National Institute of Polar Research, Tokyo, 1988, pp. 65–101.
[22] A.Y. Barkov, K.V.O. Laajoki, S.A. Gehör, Y.N. Yakovlev, O. Taikina-Aho, Chlorine-poor analogues of djerfisherite-thalfenisite from Noril'sk, Siberia and Salmagorsky, Kola Peninsula, Russia, Can. Mineral. 35 (1997) 1421–1430.
[23] H. Leroux, J.-C. Doukhan, F. Guyot, Metal-silicate interaction in quenched shock-induced melt of the Tenham L6-chondrite, Earth Planet. Sci. Lett. 179 (2000) 477–487.
[24] M. Nagamori, M. Kameda, Equilibrium between Fe-S-O system melts and CO-CO_2-SO_2 gas mixtures at 1200°, Trans. Jpn. Inst. Metals 11 (1965) 21–30.

[25] V. Kress, Thermochemistry of sulfide liquids. I. The system O-S-Fe at 1 bar, Contrib. Mineral. Petrol. 127 (1997) 176–186.
[26] G.A. Gaetani, T.L. Grove, Wetting of mantle olivine by sulfide melt: implications for Re/Os ratios in mantle peridotite and late stage core formation, Earth Planet. Sci. Lett. 169 (1999) 147–163.
[27] V. Kress, Thermochemistry of sulfide liquids. II. Associated solution model for sulfide liquids in the system O-S-Fe, Contrib. Mineral. Petrol. 139 (2000) 316–325.
[28] V. Kress, http://gneiss.geology.washington.edu/–kress/BrimstoneHomePage.html, 2000.
[29] B.J. Wood, D.G. Fraser, Elementary Thermodynamics for Geologists, Oxford University Press, Oxford, 1976.
[30] C.K. Gessmann, D.C. Rubie, Metal-oxide equilibria at high pressures and temperatures: Are Si and O the light elements in the core, Mineral. Mag. A 62 (1998) 517–518.
[31] C.K. Gessmann, D.C. Rubie, Si and O solubilities in liquid metal as a function of pressure, temperature and oxygen fugacity, in: Origin of the Earth and Moon, Lunar and Planetary Institute, Houston, TX, 1998, 10 pp.
[32] K. Righter, M.J. Drake, G. Yaxley, Prediction of siderophile element metal/silicate partition coefficients to 20 GPa and 2800°C the effects of pressure, temperature, oxygen fugacity and silicate and metallic melt compositions, Phys. Earth Planet. Inter. 100 (1997) 115–134.
[33] K. Righter, M.J. Drake, Effect of water on metal-silicate partitioning of siderophile elements: a high pressure and temperature terrestrial magma ocean and core formation, Earth Planet. Sci. Lett. 171 (1999) 383–399.
[34] C.K. Gessmann, D.C. Rubie, The influence of pressure on the partitioning of Mn, Cr and V: Implications for the formation of the Earth's core, Earth Planet. Sci. Lett. 184 (2000) 95–107.
[35] V. Hillgren, C.K. Gessmann, J. Li, An experimental perspective on the light element in the Earth's core, in: R. Canup, K. Righter (Eds.), Origin of the Earth and Moon, Lunar and Planetary Institute, University of Arizona Press, Tucson, AZ, 2000, pp. 245–263.
[36] W.R. VanSchmus, Natural radioactivity of the crust and mantle, in: T.H. Ahrens (Ed.), Global Earth Physics, A Handbook of Physical Constants, AGU Reference Shelf 1, AGU, Washington, DC, 1995, pp. 283–291.
[37] G. Dreibus, H. Palme, Cosmochemical constraints on the sulfur content in the Earth's core, Geochim. Cosmochim. Acta 60 (1996) 1125–1130.